Why perfusion measurements will fail

Constantin Sandmann, Erik A. Hanson, Alexander Malyshev, Arvid Lundervold, Jan Modersitzki, Erlend Hodneland

***Abstract*—In perfusion imaging the usage of traditional one-compartment models to estimate hemodynamic parameters like blood flow (perfusion), blood volume and mean transit times is widespread. In this paper we show limits of traditional models to recover perfusion in coupled systems. Based on modeling of porous media flow, we introduce a continuous model for propagation of a tracer in the capillary tissue. We show that the proposed model can be understood as a coupled set of traditional one-compartment models. It is furthermore demonstrated that traditional models (deconvolution, maximum slope) are accurately recovering the perfusion if applied to the full system. However, it is shown both analytically and experimentally that results of traditional models are not meaningful if applied only to smaller portions of the system, and will result in overestimation of perfusion. Evidence of real patient data is provided, indicating that this effect might also be observed in real-life applications. As a remedy, we propose to define perfusion mathematically in coupled systems as laminar flow along the streamlines.**

I. Introduction

Quantitative measurements of hemodynamic medical parameters based on tracer kinetic modeling are widespread both in research and in clinical practice [1]. In the present work, we focus on mathematical models to estimate blood perfusion (cerebral blood flow, CBF), blood volume (cerebral blood volume, CBV), and mean transit time (MTT) of the brain from contrast-enhanced dynamic image data.

While hardware limitations in medical imaging for decades have confined studies to only handle larger tissue regions or full organs, modern imaging technology and voxel based analysis give rise to aspirations about detailed perfusion maps with sub-millimeter precision. Examples of estimated parameter maps are found in i.e. [2], [3]. Quantitative perfusion maps, as well as other parameter maps arising from tracer kinetic modeling, can be combined with anatomical information, and the maps have proven to be of particular value in e.g. stroke studies for localization of trauma. Among the physiological parameters obtainable from tracer kinetic models, CBF has proven to be particularly difficult to reliably describe on a voxel-basis [4]. Causes for these limitations in perfusion estimations are issues in the numerical implementation [4], but might also depend on over-simplified dynamic models, which were originally designed to describe larger volumes of interest [5]. Even though voxel wise perfusion measurements are difficult to establish, examples of perfusion maps are extensively reported in the literature [2], [3].

There have been several approaches to clarify the concept of perfusion in a continuous sense. In [6], dispersion of the arterial input function was simulated using Navier-Stokes equations. It was shown that neglecting to account for dispersion can have adverse impact on perfusion measurements. More recently, a mathematical theory for voxelwise perfusion was introduced in [7] as an alternative to the traditional region of interest (ROI) based models. However, evaluation of the proposed modeling is still pending.

In this work we focus on the validity of traditional perfusion models. We do this by simulating a tissue patch with one inlet, one outlet, and a highly developed capillary system in between. A directional flow field for the patch is set up according to Darcy's law from porous media flow [8], assuming that blood flow is mainly driven by pressure differences. After that, contrast agent propagation in this patch is simulated using standard transport equations.As a result, we show that the resulting 3D system can be equivalently described by a coupled set of multiple traditional one-compartment models, in line with the physical environment where each control volume is feeding the direct neighbors.

We then proceed to demonstrate that traditional models like deconvolution or maximum slope are able to recover the perfusion accurately if applied to the whole system. However, when applying the traditional models to isolated parts of the full system, we find that local perfusion in coupled systems is not straight-forward to define. In order to cope with this issue, two possible definitions of voxel-wise perfusion are presented: A definition P_{v} which is closely connected to the concept of local arterial input functions and a tailored definition for continuous models P_{s}.

Our results show that perfusion results from traditional models tend to overestimate P_{s} and to underestimate P_{v} if they are applied only to parts of the full system. Analytic results are given, which show that the recovered perfusion depends on all upstream flow and not only on the local value. We also show results indicating that overestimation of perfusion due to coupling might also be found in real data.

In light of expected improvements in spatial resolution of medical scanners, traditional models will increasingly fail to accurately measure blood-flow when applied to patches of the capillary system. Instead, this establishes the need for continuous models as e.g. proposed in [7].

II. Traditional Models for perfusion

In this section we describe the convolution- and the maximum slope model, two widely used one-compartment pharmacokinetic models for measurements of CBF and CBV. These models were chosen for investigating the behaviour of traditional indicator dilution theory at finer scales. For the remaining, they are referred to as *traditional* models.

Let Ω_i be an arbitrary control volume with one inlet and one outlet, and let $C(t)$ denote the average CA concentration within Ω_i at timepoint t. The traditional model assumes that the change of concentration at timepoint t can be described by

the ordinary differential equation $C'(t) = P_{\mathrm{a}} c_{\mathrm{a}}(t) - P_{\mathrm{v}} c_{\mathrm{v}}(t)$. Here $c_{\mathrm{a}}, c_{\mathrm{v}}$ are the CA plasma concentrations at the inlet and outlet of Ω_i, and $P_{\mathrm{a}}, P_{\mathrm{v}}$ are the corresponding perfusion values at these locations. Assuming incompressible flow leads to $P_{\mathrm{a}} = P_{\mathrm{v}}$ and hence we obtain the general form

$$C'(t) = P_{\mathrm{a}} \left(c_{\mathrm{a}}(t) - c_{\mathrm{v}}(t) \right). \tag{1}$$

In the following it is assumed that the plasma tracer concentration c_{a} at the inlet is known. In clinical practice this can be implemented by measuring c_{a} directly in a feeding artery [9]. Since c_{v} is usually unknown, additional assumptions need to be made if one wants to reconstruct P_{a} from a given tissue curve C. The convolution model and the maximum slope (MS) model diverge in further assumptions.

A. The Convolution Model

For the deconvolution model, one approach is to assume there is an unknown probability distribution of transit times h through Ω_i. This leads to

$$c_{\mathrm{v}}(t) = (h * c_{\mathrm{a}})(t) := \int_0^t c_{\mathrm{a}}(s) h(t-s) \, \mathrm{d}s. \tag{2}$$

Combining this with (1) yields $C'(t) = P_{\mathrm{a}} c_{\mathrm{a}}(t) - P_{\mathrm{a}}(h * c_{\mathrm{a}})(t)$. Integrating this equation and using basic properties of the convolution one obtains the general solution

$$C(t) = (I * c_{\mathrm{a}})(t). \tag{3}$$

where the *impuls-response function* I is defined as $I(t) := P_{\mathrm{a}}(1 - \int_0^t h(s) \, \mathrm{d}s)$. The task of identifying $I(t)$ given a tissue curve $C(t)$ and an arterial input function $c_{\mathrm{a}}(t)$ is a deconvolution problem. If $I(t)$ is recovered, P_{a} can subsequently be estimated as $P_{\mathrm{a}} = \max_t I(t)$. There are several methods to perform the deconvolution. A standard approach using Fourier-based algorithms is sensitive to the presence of noise [9]. Another class of deconvolution algorithms gaining increasing attention are based on Bayesian modeling [10]. However the numerical handling is still difficult since complex and error-prone numerical integration has to be performed [10]. A popular class among deconvolution algorithms is based on singular value decomposition (SVD) [9]. These algorithms have shown to be robust for a reasonable noise level. Also, they can be easily adapted to be robust against delays in tracer arrival using block-circular structures (bSVD cf. [11]). In order to identify the impuls-response function $I(t)$ from simulated data, we hence decided to use the bSVD model as proposed in [11].

B. The Maximum Slope Model

In the MS model it is assumed that when c_{a} has its maximum, only a negligible amount of CA is leaving the system [12]. For this time interval, (1) reduces to

$$C'(t) = P_{\mathrm{a}} c_{\mathrm{a}}(t), \tag{4}$$

in case one can see that if c_{a} has a maximum, also C' must have a maximum since stationarity in P_{a} is assumed. Hence, it holds that

$$P_{\mathrm{a}} = \frac{\max_t C'(t)}{\max_t c_{\mathrm{a}}(t)}. \tag{5}$$

III. A Synthetic Model for Capillary Flow

The validity of the traditional methods rely on a ROI having only one inlet and one outlet, and that transition times are prescribed by some probability distribution. In fact, the assumption of one inlet and one outlet may easily be violated when we locally describe CA propagation through a larger area with a highly developed capillary system. For this type of model system we expect instead a set of coupled equations where each voxel can be regarded as an inlet for surrounding voxels. Hence, in order to make a realistic synthetic model for capillary flow, we decided to describe the CA propagation as a spatially coupled transport process, i.e. using partial differential equations (PDE) for transport. This PDE model is used for validation of the traditional models.

Assuming stationary, incompressible flow at low Reynold numbers within the capillary system [13], the flow can be described by Darcy's law [8]. For simplicity, we also assume an isotropic porous media. A major difference between the described flow-model model and traditional tracer kinetic modeling is the normalization of the flow field within the traditional models, using volume normalized fluid flow with units [mm^3/s/mm^3], referred to as perfusion, as a quantity to describe fluid transport. However, to avoid a discretization dependent flow field, for the PDE model we instead use vector valued surface fluid flux $q = q(x)$ with units [mm^3/s/mm^2], in agreement with geoscience and porous media simulation theory. The fluid flux is a vector field describing the volume of fluid per unit time flowing across a sliced unit area of the sample. Apart from the normalization with respect to surface, the assumptions of linearity and stationarity in the fluid flux are in complete agreement with standard pharmacokinetic modeling [1].

A. Modelling Capillary Blood Flow

For the time being we will not consider the contrast agent concentrations, but the fluid flow in general. The fluid density ρ [mg/mm^3] is denoted by $\rho = \rho(x,t)$. The flux q as well as the porosity ϕ [mm^3/mm^3] are assumed to be stationary and hence independent of time. Fluid entering and leaving the system is described by a source- and sink term $\tilde{Q} = \tilde{Q}(x)$ [mg/s/mm^3]. The continuity equation describing conservation of fluid mass states

$$\frac{\partial(\phi\rho)}{\partial t} + \nabla \cdot (\rho q) = \tilde{Q}. \tag{6}$$

Furthermore, assuming that the fluid flow is steady-state and that the density of blood ρ is constant in space, we obtain $\nabla \cdot q = \tilde{Q}/\rho$. In order to scale away the density ρ we define another source term Q [mm^3/s/mm^3] having the relation $\tilde{Q} := Q\rho$, thus transforming the equation into

$$\nabla \cdot q = Q \tag{7}$$

where the right hand side is a volume flux, only non-zero within the source or the sink locations. Elsewhere, (7) is concurrent with divergence free flow of an incompressible fluid.

Low velocity fluid flux in porous media is usually assumed to be driven by pressure differences and described by Darcy's law in the absence of gravitational forces [8]

$$q = -\frac{\mathbf{k}}{\mu}\nabla p. \tag{8}$$

Here $\mathbf{k}$ [mm^2] is the permeability tensor, p [Pa] is the pressure, and $\mu = \mu(x)$ [kPas] is the viscosity of the fluid. We will assume that $\mathbf{k}$ is a symmetric and positive definite tensor with only nonzero diagonal elements $\mathbf{k}_{ii} = k$. Equations (7) and (8) can be combined, yielding the following elliptic partial differential equation in the pressure-field p,

$$\left| \begin{aligned} \nabla \cdot \left(-\frac{\mathbf{k}}{\mu}\nabla p \right) &= Q \qquad && x \in \Omega, \\ n \cdot \nabla p &= 0 && x \in \partial\Omega \end{aligned} \right| \tag{9}$$

where we also added Neuman boundary conditions reflecting zero fluid flux $q(x)$ across $\partial\Omega$. Here, $\partial\Omega$ denotes the boundary of Ω and n the outward unit normal vector. Note that (9) defines a solution which is only unique up to constant [15]. After solving (9), the flux field can be computed according to (8) from the obtained pressure map.

B. Modelling Indicator Dilution

In Section III-A we introduced a model describing blood flow through fluxes and pressure fields. The introduced framework does not relate flow to propagation of a contrast agent. This section describes a model for CA propagation in the tissue as it is dissolved in the evolving fluid. We assume that the CA is entering the domain along with the fluid flowing in via the source, and similarly extracted at a sink. The resulting CA concentration map is a simulation of the CA concentration one would observe within real MRI measurements.

In order to define meaningful and continuous contrast agent concentrations, we first describe the average CA concentration in an (arbitrarily) small tissue volume Ω_i where $C_i(t) := C(x_i, t)$ and $\phi_i := \phi(x_i)$ are assumed to be constant within Ω_i. Assume that V_i is the volume of Ω_i and v_i the the blood volume within Ω_i. By definition, porosity reflects the relative space within the vascular system, and is given by $\phi_i = v_i/V_i$. Let $C_i(t)$ denote the CA concentration in Ω_i with respect to the whole volume V_i at timepoint t. The CA concentration with respect to the blood volume v_i is denoted by $c_i(t)$. From the definition of c_i, C_i and ϕ_i we obtain the relation $C_i(t) = \phi_i c_i(t)$. The rate of change of tracer molecules within the control volume Ω_i can he phrased as

$$\frac{\mathrm{d}}{\mathrm{d}t}\int_{\Omega_i} C_i(t)\,\mathrm{d}x = \int_{\Omega_i} \frac{\mathrm{d}}{\mathrm{d}t}(\phi_i c_i(t))\,\mathrm{d}x = \int_{\Omega_i} \phi_i \frac{dc_i}{dt}\,\mathrm{d}x. \tag{10}$$

where the assumption of stationary ϕ_i was used. Since we expect mainly transport and marginal diffusion, the change in tracer mass within Ω_i occurs only from advective flow and the source and sink field Q. Let us write the source- and the sink term as $Q = Q_{\mathrm{si}} + Q_{\mathrm{so}}$ where $Q_{\mathrm{si}} < 0$ is the sink and $Q_{\mathrm{so}} > 0$ is the source, and zero elsewhere. Both are assumed to be zero everywhere except at in the respective source and sink locations. Note that $\int_\Omega Q\,\mathrm{d}x = 0$. The change in contrast agent at time point t from fluid entering the control volume can be written as

$$-\int_{\partial\Omega_i} c_i(t)(q_i \cdot n)\,\mathrm{d}s + \int_{\Omega_i} c_{\mathrm{a}}(t) Q_{so,i}\,\mathrm{d}x + \int_{\Omega_i} c_i(t) Q_{si,i}\,\mathrm{d}x, \tag{11}$$

where n is the outward unit normal on $\partial\Omega_i$. In standard pharmacokinetic modeling, c_{a} is referred to as the arterial input function (AIF). From the principle of conservation of tracer molecules, equations (10) and (11) must balance for each control volume Ω_i, such that

$$\begin{aligned} &\int_{\Omega_i} \phi_i \frac{dc_i}{dt}\,\mathrm{d}x + \int_{\partial\Omega_i} c_i(t)(q_i \cdot n)\,\mathrm{d}s \\ &= \int_{\Omega_i} c_{\mathrm{a}}(t) Q_{so,i}\,\mathrm{d}x + \int_{\Omega_i} c_i(t) Q_{si,i}\,\mathrm{d}x. \end{aligned} \tag{12}$$

Now, let the contrast agent concentrations, porosity, volume fluxes, and surface flux be continuous functions of space and time. Equation (12) is then consistent with the continuity equation on local form

$$\left| \begin{aligned} \phi\frac{\partial c}{\partial t} + \nabla \cdot (cq) &= c_{\mathrm{a}} Q_{\mathrm{so}} + c Q_{\mathrm{si}} && x \in \Omega,\ t > 0, \\ c(x,t) &= 0 && x \in \Omega,\ t = 0. \end{aligned} \right| \tag{13}$$

where we also added the initial value $c(x, 0) = 0$ to ensure uniqueness. Equation (13) is a linear transport equation in $c(x, t)$. Following [15], equation (13) admits a unique local solution.

C. Relating the transport equation model with the traditional deconvolution model for perfusion

In this section we will describe how the continuous model is related to the traditional deconvolution model. More specifically, we will show that in the continuous model each voxel can be described by a traditional model with arterial input determined by the adjacent upstream voxels. Additionally, we will consider the effect of deconvolving a voxel curve C_i of the continuous model with the global arterial input function c_{a} of the tissue. We will show that in this case the resulting residue function will depend on the perfusion of all upstream voxels. Note that this effect makes the application of standard deconvolution techniques difficult in coupled systems, since perfusion results will depend on the flow in feeding tissue.

Let us start by modeling the CA concentration in a given voxel using traditional models. Let us consider the continuity equation for one voxel (12). For sake of simplicity let us assume that $Q_{\mathrm{so},i} = Q_{\mathrm{si},i} = 0$. Note that it is possible to extend the following approach also to voxels where $Q_{\mathrm{so},i} \neq 0$ or $Q_{\mathrm{si},i} \neq 0$. We will now show that (12) can equivalently be described as a traditional one-dimensional equation for a well-mixed compartment. First, let us define the areas of inflow and outflow over the boundary by $S_{\mathrm{in}} := \{x \in \partial\Omega_i : q_i(x) \cdot n(x) < 0\}$ and $S_{\mathrm{out}} := \{x \in \partial\Omega_i :\ q_i(x) \cdot n(x) > 0\}$ respectively. In order to define a single arterial input rather than an arterial input which depends on the location, we define c_{in} as a weighted average of the concentrations at the boundary:

$$c_{\mathrm{in}}(t) := \frac{\int_{S_{\mathrm{in}}} c(t)(q_i \cdot n)\,\mathrm{d}s}{\int_{S_{\mathrm{in}}} q_i \cdot n\,\mathrm{d}s} \tag{14}$$

We now define the perfusion of the voxel Ω_i as follows:

$$P_{\text{in}} := \frac{-1}{\text{Vol}(\Omega_i)} \int_{S_{\text{in}}} q_i \cdot n \, \mathrm{d}s, \quad P_{\text{out}} := \frac{1}{\text{Vol}(\Omega_i)} \int_{S_{\text{out}}} q_i \cdot n \, \mathrm{d}s \tag{15}$$

Let us now assume that the flow-field q is divergence-free and the amount of CA entering the region is the same as the amount of CA leaving it. Then it holds that $P_{\text{in}} = P_{\text{out}}$ and hence equation (12) can be reformulated as

$$(\phi_i c_i)'(t) = P_{\text{in}}(c_{\text{in}}(t) - c_{\text{out}}(t)). \tag{16}$$

Note that in the discretization described in Section III-B it is assumed that the CA concentration at the outflow S_{out} equals the concentration within the voxel and that the concentration at the inflow is the concentration at the adjacent voxels. In this case In this case it follows that (16) reduces to standard equation for a well-mixed compartment $C_i'(t) = P_{\text{in}}(c_{\text{in}}(t) - c_i'(t))$ with solution

$$C_i(t) = (I_i * c_{\text{in}})(t) \text{ for } I_i(t) = P_{\text{in}} e^{-P_{\text{in}}/\phi_i t}. \tag{17}$$

c_{in} is determined by (14) and the adjacent upstream voxels. To verify this relationship also numerically, we simulated a tissue curve C_i using the continuous model and using (17). Both curves matched up to numerical numerical errors perfectly, cf. Figure 1 a).

As a direct consequence it follows by recursion that for a given voxel at location i the concentration can be written as a convolution of the (global) arterial input function with the impuls-response functions of all upstream voxels, i.e.

$$C_i(t) = \phi_i((I_1 * \cdots * I_l) * c_{\text{a}})(t).$$

where $I_j(s) := p_i \exp(-p_i(s))$ and $p_i = P_i/\phi_i$. Following [**?**], the convolution of exponential functions with pairwise different parameters p_i is given by

$$(I_1 * \cdots * I_n)(s) = \sum_{i=1}^{n} \frac{\Pi_{j=1}^{n} p_j}{\Pi_{j=1, j\neq i}^{n} (p_j - p_i)} e^{-p_i s}, \tag{18}$$

see [**?**] for the case $p_i = p_j$ for some i, j. Again we also verified this relationship experimentally: Figure 1 b) shows the impuls response function determined by (18) and the impuls response function obtained from deconvolving a tissue curve I_i of the continuous model with the arterial input function. Again both function coincide perfectly.

D. Converting Flow to Perfusion

The model described in (9) uniquely determines the flux field $q(x)$. However, in pharmacokinetic modeling the parameter of interest is usually the CBF, which we will denote by $P(x)$ as the voxel wise field of perfusion. The surface flux and perfusion are physically distinct, and there are at least two differences between $q(x)$ and $P(x)$. First, the flux is a vector field and the perfusion is a scalar field. Second, the flux is normalized to a surface area and the perfusion is normalized to a volume. Thus, the surface flux and the perfusion are strictly, mathematically different but still conceptually related. In the following we describe a method for converting flux into perfusion, motivated by the need to compare the ground-truth flux field to the scalar valued perfusion field obtained by traditional methods.

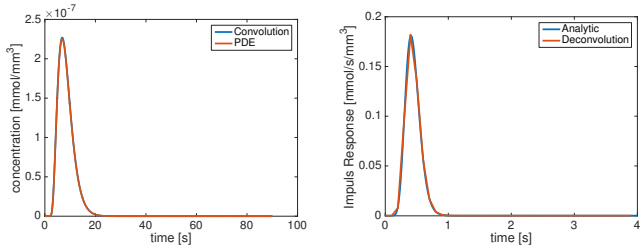

Figure 1. a) Tissue curve of the 2D phantom at location [32,35]. Simulation using (17) with $P_i = 5328$ ml/min/100ml and c_{in} taken locally from upstream voxels in blue. The simulation using the continuous model is given in red. Curves are coinciding perfectly. Note that the perfusion is unrealisticly high since normalization is performed with respect to the volume of one voxel. b) Impuls response functions at location [1,20] for the global arterial input function. The analytic function given by (18) is displayed in blue, the function recovered by deconvolution is displayed in red. As outlined in Section III-C both functions are coinciding perfectly. Note that the recovered impuls-response function depends on the perfusion of all upstream voxels and not only the adjacent voxels.

The common understanding of perfusion or volume flux $P(x)$ is the amount of blood feeding a tissue volume per unit time, with units [mm^3/s/mm^3]. One obvious approach for converting flux into perfusion could be to estimate the perfusion as the total inflow (or outflow) of fluid (e.g. arterial blood) into a control region per unit time, and then normalizing with the control region volume. This is a valid approach only if the control regions are not feeding each other, and is therefore well-founded for the entire organ. Such understanding of perfusion is in line with the theoretical foundation of traditional compartment models for perfusion where a control region has its own source of feeding arterial blood, independent of the neighbor regions.

On the other hand, if the control region is a single voxel or a sub-division of an organ with sequentially feeding arterial blood, the traditional model assumptions are violated since every control region will feed its neighbours, thus becoming a coupled system of flow. Simply summing the total inflow into a voxel and dividing by the voxel volume will strongly over-estimate the perfusion since the normalization would refer to the wrong volume. This phenomenon is demonstrated in Fig. 2 where the volume on the left has the true perfusion of $P_1 = F_0/(2V)$ for an incoming flow F_0 [mm^3/s] and distribution volume $2V$ [mm^3]. However, for another discretization as shown in the middle, the perfusion within each of these sub-volumes becomes $P_2 = F_0/V = 2P_1$. Taking the average across the two sub-volumes, it is clear that the perfusion is over-estimated with a factor of two. A discretization dependent perfusion estimate is not recommendable, and the perfusion estimate of P_2 is clearly wrong.

In the following paragraph will introduce a meaningful notion of perfusion for the continuous model. To do this, we will consider distribution volumes which are following the streamlines. For each point of a streamline we will select a small perpendicular disk with radius chosen in such a way that the total flow over each disk is constant along the streamline.

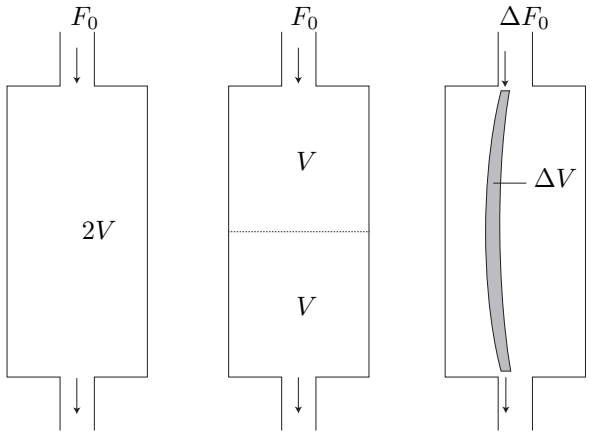

Figure 2. Perfusion within a small volume. Left: A compartment with volume $2V$ is exposed to a flow F_0 [mm^3/s] of fluid. By definition, the perfusion within this compartment becomes $P_1 = F_0/(2V)$. Middle: The same volume is divided into two compartments (e.g. voxels), and the perfusion for each of the compartments becomes $P_2 = F_0/V = 2P_1$. The discrepancy between the two discretizations occurs because the flow is counted twice as it is fed from one voxel to the other. Right: As a solution to the described problem we rather pick out a true distribution volume ΔV (area in this 2D sketch), which is a small area around a given streamline along the centre line of the grey area. This is the true distribution volume (area in this 2D sketch) which is fed with arterial blood from the incoming fractional flow ΔF_0. The correct perfusion within ΔV is therefore $\Delta F_0/\Delta V$. The entire compartment can further be divided into similar infinitesimal distribution volumes, thus providing locally correct perfusion estimates.

This disks will form a small tube around the streamline with constant flow over each cross-section. Since the total flow over each disk is constant, we can define the perfusion for each voxel by the traditional model, obtaining a perfusion value which is constant along the streamline. To obtain a truly local perfusion, we will let the radii of the disks go to zero.

More precisely, let us consider an arbitrary streamline $S \subseteq \Omega \subseteq \mathbb{R}^3$ of length $l > 0$ and parametrization $s : [0, l] \to \Omega$. We start by calculating the total flow over a small 2-D disk which is perpendicular to the streamline. Let $y \in S$ be an arbitrary location along the streamline. The total flow over a 2-D disk $B_r(y)$ perpendicular to the flow-field $q(y)$ is given by

$$F(y, r) = \int_{B_r(y)} q(x) \cdot \nu \, \mathrm{d}x \text{ where } \nu := q(y)/|q(y)|.$$

In order to calculate the perfusion, we need to establish the volume of a small tube around the streamline. We will not consider a tube with constant radius, but one with spatially varying radii $p : S \to \mathbb{R}^+$. The total volume of such a tube surrounding the streamline is given by

$$V(p) = \int_0^l p^2(s(u))\pi \, \mathrm{d}u$$

We define the perfusion at an arbitrary point $y \in S$ by

$$P(y) := \lim_{\varepsilon \to 0} \frac{F(y, \varepsilon p(y))}{V(\varepsilon p)} \text{ for } p(x) := 1/\sqrt{|q(x)|}.$$

Note that the radii $p(x)$ are chosen in such a way that in the limit $\varepsilon \to 0$ the total flow is constant along the streamline. To see this, let us assume that q is differentiable with Jacobian J. Using a Taylor expansion of $q(x)$ around y as well as a change of coordinates yields

$$F(y, \varepsilon r) = \varepsilon^2 \Big(\pi + \varepsilon \int_{B_1(0)} \nu^\top J(\zeta) \, \mathrm{d}x \Big)$$

where $\zeta \in (0, x)$ and simplifications are due to $r = p(y) = 1/\sqrt{|q(y)|}$ and $\nu := q(y)/|q(y)|$. Note that since $V(\varepsilon p) = \varepsilon^2 V(p)$ it follows that

$$P(y) = \frac{\pi}{V(p)} \tag{19}$$

Equation (19) is independent of the spatial location y and an explicit formula for converting flux into perfusion.

E. A Method to Estimate local Porosity

It is known from literature on traditional models for perfusion that CBV for the entire compartment can be expressed as

$$\phi = \frac{\int_0^\infty C(t) dt}{\int_0^\infty c_a(t) dt}. \tag{20}$$

where $C(t)$ are the tracer concentration with respect to a well mixed compartment and $c_a(t)$ is the tracer plasma concentration of the arterial input. However, it is not obvious that (20) is valid also for a continuous field model where the voxels are feeding each other. We will now proof that (20) is nevertheless valid.

Returning to the local definition of fluid tracer concentration as $c(x, t)$, the PDE in (13) is consistent with

$$\phi \frac{\partial c}{\partial t} = -q \cdot \nabla c. \tag{21}$$

for locations x where $Q(x) = 0$. Integrating from t_0 to t_1 results in the model

$$\phi[c(x, t_1) - c(x, t_0)] = -\int_{t_0}^{t_1} q \cdot \nabla c \, \mathrm{d}t. \tag{22}$$

Approaching the limit $t_0 = 0, t_1 = \infty$, using the boundary conditions $c(x, 0) = c(x, \infty) = 0$ and defining $E(x) := \int_0^\infty c(x, t) \, \mathrm{d}t$ leads to

$$0 = q \cdot \nabla E(x). \tag{23}$$

We can interpret this equation such that q is tangent to the level-sets of the function $E(x)$, which means that $E(x)$ is constant along the streamlines of the fluid flow. Since at the beginning of the streamline it holds by construction that $c(x_0, t) = c_\mathrm{a}(t)$ and since $C(x, t) = \phi(x)c(x, t)$ it follows that

$$\phi(x) = \frac{\int_0^\infty C(x, t) \, \mathrm{d}t}{\int_0^\infty c_\mathrm{a}(t) \, \mathrm{d}t}. \tag{24}$$

Note that equation (24) coincides with the traditional formula (20) for ϕ.

IV. Numerical Experiments

Based on the field modes described in Section III, we now establish an experimental setup suited to study the performance of the deconvolution methods in a synthetic flow field with a known ground truth.

Based on (9) and (13) we set up a forward simulation of blood-flow and indicator dilution through the capillary system. We aimed at creating a transparent synthetic test case and kept all optional parameters as simple as possible.

We chose a standard arterial input function [9], the gamma-variate function

$$c_{\mathrm{a}}(t) := D_0(t-t_0)^{\alpha} e^{-(t-t_0)/\beta} \tag{25}$$

for default parameters $\alpha = 3$, $D_0 = 1$, $\beta = 1.5\,\mathrm{s}$ and $t_0 = 0\,\mathrm{s}$. Ground truth perfusion for the domain of size $3\,\mathrm{mm} \times 3\,\mathrm{mm} \times 1\,\mathrm{mm}$ was chosen $50\mathrm{ml/min/100ml}$. The source term was assigned to the upper left voxel and the sink term was assigned to the lower right voxel. It was assumed that both the domain of inflow as well as outflow were approximately of the voxel-size, leading numerically to Delta-like source and sink terms Q_{so} and Q_{si}. Permeability was chosen isotropic and constant throughout the domain $\mathbf{k} = 5 \times 10^{-6}\,\mathrm{mm}^2$, assuming no directional bias of the capillary system. Dynamic blood viscosity was chosen $\mu = 5 \times 10^{-6}\,\mathrm{kPas}$ according to [16]. Porosity (e.g. CBV) was assumed to be $\phi = 0.05\,\mathrm{mm}^3/\mathrm{mm}^3$. Since our aim was to test limits of established methods and to simulate high resolution scans, a voxel size of $(0.05\,\mathrm{mm}, 0.05\,\mathrm{mm}, 3\,\mathrm{mm})$ was assumed. The flow field visualized in Figure 3 (b) is vector flux integrated across cell surface, $\int_{\partial\Omega_{ij}} q\,\mathrm{d}s$ with units $[\mathrm{mm}^3/\mathrm{s}]$.

Equation (9) was solved numerically using the two-point flux-approximation method widely used in reservoir mechanics [14]. The transport described in (12) was implemented using first order upwinding [17], yielding a 4D CA concentration map $C_{i,j} = c$. From the porous media model using (9) and (13), streamlines were found from tracking of the flux vector field q, using a method closely related to FACT [18] used for tracking within DTI (Diffusion Tensor Imaging) for tractography.

V. Results

A. Reconstruction of perfusion within synthetic data

We tested the convolution based traditional model (bSVD) (3) as well as maximum-slope (MS) model (5) for their capability to recover the perfusion values. Prior to reconstruction, the CA concentration map $C(x,t)$ was downsampled to a time-resolution of $0.2\,\mathrm{s}$ in order to stay within comparable time sampling existing on modern MR equipment for dynamic imaging. In order to simulate different spatial resolutions of the scanning process, the data was averaged using different block-sizes ranging from $(1,1)$ pixel to $(64,64)$ pixels. Success of restoration was measured in terms of the relative error of the recovered perfusion with respect to the ground truth perfusion, $RE := |P_{\mathrm{rec}} - P_{\mathrm{true}}/P_{\mathrm{true}} \cdot 100\%$. The recovered perfusion was compared against the two perfusion maps depicted in Figure 3:

Perfusion map P_{v} was set up using the local definition definition (15). Since normalization is performed with respect to voxel size, the values are unrealistically high and will vary with the discretization. As equation (17) shows, this can nevertheless be regarded a valid definition of perfusion since it models effects of a local arterial input function. To quantify the errors occuring by using a different arterial input function, in the experiments the global arterial input function was used for the deconvolution, cf. (18). Since the corresponding impuls response functions are decaying rapidly, this makes the deconvolution especially sensitive to downsampling of the time-curves..

The perfusion map P_{s} was set up using the definition along the streamlines (19). This definition most accurately reflects the physical perfusion at a given location and shows plausible perfusion values, cf. Figure 3. However, we do not expect the traditional models to be able to recover these values accurately. Errors are given to indicate the amount of overestimation by standard methods.

Results are displayed in Table I. For the complete system, both the maximum slope method and the convolution method could restore the ground truth perfusion of $50\,\mathrm{ml/min/100ml}$ accurately with errors of $< 1\%$ and 4% respectively. However, this changes if the methods are applied only to parts of the system. If compared to P_{v}, one can see that results are clearly improving with increasing block size. Also a clear advantage of the bSVD method as compared to MS can be observed. This is possibly to the additional assumptions of the MS method. If compared to P_{s}, rendering both methods incapable to recover the physically more meaningful notion of perfusion along the streamlines.

Results from reconstructing ϕ are shown in also shown in Table I, where the relative errors are low for both forward data generated by the transport equation as well as the convolution model. This is supported by the analytic considerations in Section III-E.

Table I
Relative error RE (%) for reconstructing perfusion P_{v}, P_{s} and the blood-volume ϕ. Displayed is the median RE. Both reconstruction models MS and bSVD are able to restore the perfusion for the entire domain, but fail for smaller block sizes. For larger block-sizes the bSVD model restores the perfusion more accurately than the MS model. However, the blood volume ϕ is recovered accurately. For a more detailed discussion see Section V-A.

	P_{v}		CBV	P_{s}	
block size	bSVD	MS		bSVD	MS
(1,1)	93%	98%	<1%	423%	95%
(5,5)	67%	90%	<1%	387%	90%
(10,10)	44%	79%	<1%	292%	82%
full	4%	<1%	<1%		

The results strongly support the usage of traditional compartment models for regions which are fed directly by the measured arterial input. They also show show that if traditional models are applied only to parts of the system, they tend to overestimate the actual perfusion. Note that taking local arterial input functions is no remedy for this problem, since the resulting perfusion will depend heavily on the voxel size and overestimate the actual flow, cf. Figure 2 and equation

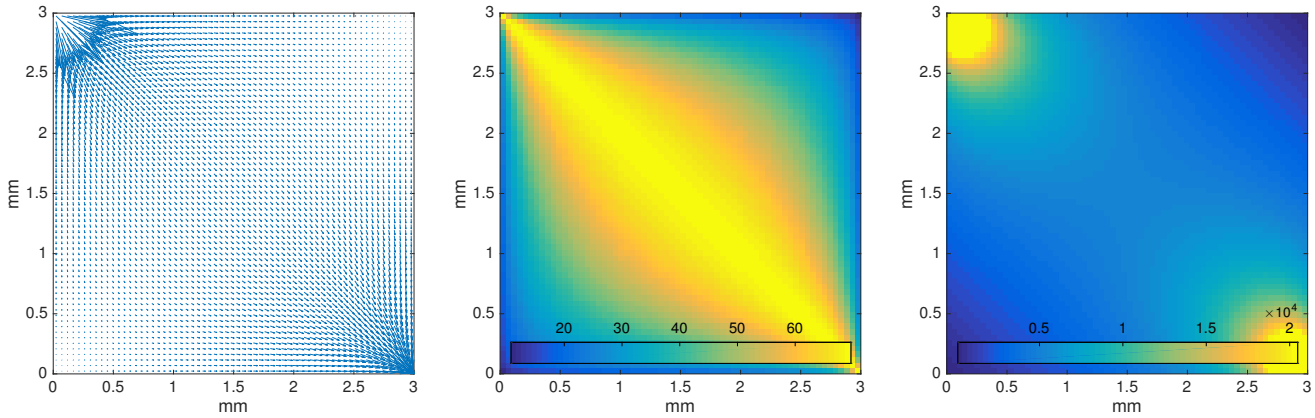

(a) Flow field (b) Perfusion P_{s} along the streamlines (c) Local perfusion P_{v}.

Figure 3. Porous media (PM) flow model with a source in the upper left corner and a sink in the lower right corner. (a) Flow field used to simulate the contrast agent, (b) Perfusion along the streamlines according to (19), (c) Local perfusion according to (15).

(17). In fact, in the described extreme example we have measured overestimations of up to 423% . All these results are supported by the real-data experiments, where we showed local overestimation of perfusion for small voxel-sizes as compared to an averaging of concentrations for the whole volume of interest. Regarding the CBV estimates, one can observe from Table I estimation of blood volume is far more stable. Even various block sizes had little impact on the results. These results are in well agreement with the analytical observations described in Section III-E, stating that equation (20) is valid for entire organs as well as for single voxels. Thus, these results support the usage of (20) for computing the CBV with high accuracy for any type of block size, including single voxels.

B. Reconstruction of perfusion within real data

Experimental results from Section V-A indicate that application of the deconvolution model to patches of tissues violating the model assumptions would lead to overestimation of blood-flow as compared to the overall flow within the volume of interest. In order to validate this guess, we applied the deconvolution model to a clinically acquired human perfusion CT dataset of a 56 years old male male admitted with suspicion of stroke to the Radboud University Medical Center in Nijmegen, the Netherlands. The perfusion scan was obtained using a Toshiba Aquilon ONE scanner, pixel-size $0.43\,\mathrm{mm} \times 0.43\,\mathrm{mm}$, slice thickness $0.5\,\mathrm{mm}$, contrast agent $50\,\mathrm{mL}$ Xentix 300, total scan-time $114\,\mathrm{s}$, time resolution ranging from $2.1\,\mathrm{s}$ in the early- to $30\,\mathrm{s}$ in the late phase of CA uptake. The arterial input function was manually selected by a medical expert within the middle cerebral artery. Since we expected to see local overestimation effects mainly for small voxel sizes, the data was processed at full resolution $(512 \times 512 \times 320)$. However, in order to deal with noise effects it was necessary to apply a prior gaussian smoothing with standard deviation of 1 voxel. Relative concentrations were estimated from the CT signal assuming a spatially independent proportionality constant. CBF was then estimated voxel-wise using a Matlab implementation of bSVD, yielding an average CBF of $64.357\,\mathrm{ml/min/100ml}$. After that, we estimated the perfusion for the whole volume of interest by averaging the concentration values first and then performing the bSVD, yielding a total CBF of $24.791\,\mathrm{ml/min/100ml}$. Results are depicted in Fig. V-B

VI. Discussion

In this work we have studied the impact of an application of traditional models to perfusion reconstruction in a coupled system of 1C models. To establish ground-truth values, we have developed a novel digital phantom to simulate blood flow within a slab of tissue with a highly developed capillary system. We have shown that the discretized model can be described equivalently as a system of coupled traditional one-compartment models.

Furthermore we have introduced two possible definitions of voxel perfusion: Perfusion P_{s} models perfusion along the streamlines and most accurately models the physical notion of volume flow. However, theory and experiments show that the traditional models cannot recover this perfusion if applied in a straight-forward manner. Perfusion P_{v} has been set up based the interpretation as a coupled system. Theory and examples show that this definition does not comply with the intended physical notion since it depends heavily on the discretization. However, we have shown that traditional models would restore this value if the correct (local) arterial input function was selected. We have additionally analyzed the impact of selecting a further upstream arterial input function both analytically and experimentally. Specifically we have given an analytic expression which shows that the perfusion will depend on the flow at all upstream voxels. Experiments show, that estimations results improve if block-sizes are increasing. Estimation of CBV however has been shown to be stable.

Our results indicate the traditional models should only be used for larger computational units where the arterial input is an actual arterial input for the domain as a whole. The development of new field models for perfusion is therefore highly demanded, in line with approaches described in [7].

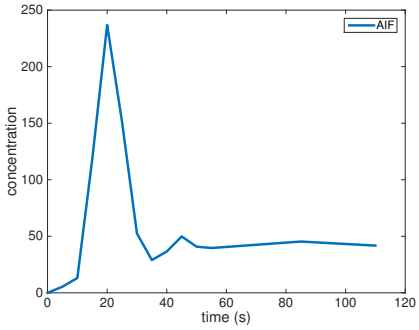

(a) Arterial input function

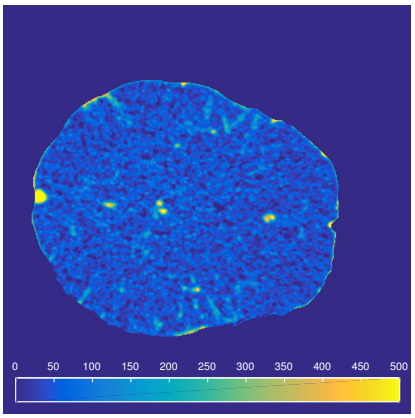

(b) One slice of the voxel-wise CBF reconstruction.

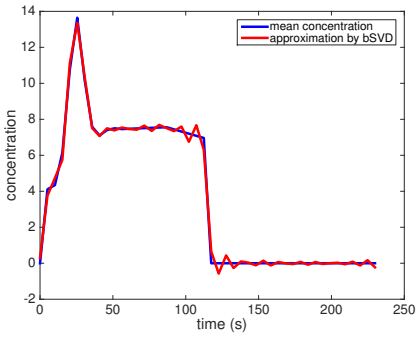

(c) mean concentration curve for the whole volume of interest and reconstruction.

Figure 4. Figure with results from the real-data experiments (see Sec. V-B for details on the data). The AIF shown in (a) was manually selected from the MCA. In (b) one slice of the voxel-wise CBF-reconstruction for a 3D volume of interest is shown. In (c) the mean-concentration curve for the complete 3D volume of interest and the approximation by bSVD is shown.

References

[1] S. P. Sourbron and D. L. Buckley, "Classic models for dynamic contrast-enhanced MRI," *NMR in Biomedicine*, vol. 26, no. 8, pp. 1004–1027, 2013.

[2] Q. Feng, X. Chen, J. Sun, Y. Zhou, Y. Sun, W. Ding, Y. Zhang, Z. Zhuang, J. Xu, and Y. Du, "Voxel-level comparison of arterial spin-labeled perfusion magnetic resonance imaging in adolescents with internet gaming addiction," *Behav Brain Funct*, vol. 9, no. 1, p. 33, 2013.

[3] Y. Chen, D. Wolk, J. Reddin, M. Korczykowski, P. Martinez, E. Musiek, A. Newberg, P. Julin, S. Arnold, J. Greenberg *et al.*, "Voxel-level comparison of arterial spin-labeled perfusion mri and fdg-pet in alzheimer disease," *Neurology*, vol. 77, no. 22, pp. 1977–1985, 2011.

[4] K. Kudo, M. Sasaki, K. Yamada, S. Momoshima, H. Utsunomiya, H. Shirato, and K. Ogasawara, "Differences in CT perfusion maps generated by different commercial software: Quantitative analysis by using identical source data of acute stroke patients 1," *Radiology*, vol. 254, no. 1, pp. 200–209, 2010.

[5] K. Zierler, "Indicator dilution methods for measuring blood flow, volume, and other properties of biological systems: a brief history and memoir," *Ann Biomed Eng*, vol. 28, no. 8, pp. 836–848, 2000.

[6] F. Calamante, P. J. Yim, and J. R. Cebral, "Estimation of bolus dispersion effects in perfusion MRI using image-based computational fluid dynamics," *Neuroimage*, vol. 19, no. 2, pp. 341–353, 2003.

[7] S. Sourbron, "A tracer-kinetic field theory for medical imaging," *IEEE Trans Med Imaging*, 2014.

[8] H. Darcy, "Les fontaines publiques de la ville de dijon," *Victor Dalmont*, p. 647, 1856.

[9] L. Østergaard, R. M. Weisskoff, D. A. Chesler, C. Gyldensted, and B. R. Rosen, "High resolution measurement of cerebral blood flow using intravascular tracer bolus passages. part i: Mathematical approach and statistical analysis," *Magn Reson Med*, vol. 36, no. 5, pp. 715–725, 1996.

[10] T. Boutelier, K. Kudo, F. Pautot, and M. Sasaki, "Bayesian hemodynamic parameter estimation by bolus tracking perfusion weighted imaging," *IEEE T Med Imaging*, vol. 31, no. 7, pp. 1381–1395, 2012.

[11] O. Wu, L. Østergaard, R. M. Weisskoff, T. Benner, B. R. Rosen, and A. G. Sorensen, "Tracer arrival timing-insensitive technique for estimating flow in mr perfusion-weighted imaging using singular value decomposition with a block-circulant deconvolution matrix," *Magn Reson Med*, vol. 50, no. 1, pp. 164–174, 2003.

[12] E. Klotz and M. König, "Perfusion measurements of the brain: using dynamic CT for the quantitative assessment of cerebral ischemia in acute stroke," *Eur J Radiol*, vol. 30, no. 3, pp. 170–184, 1999.

[13] Y.-I. Cho and D. J. Cho, "Hemorheology and microvascular disorders," *Korean circulation journal*, vol. 41, no. 6, pp. 287–295, 2011.

[14] T. G. J. E. Aarnes and K.-A. Lie, *An introduction to the numerics of flow in porous media using Matlab*. Springer Verlag, 2007.

[15] L. Evans, *Partial differential equations*, 2nd ed. Providence, Rhode Island: American Mathematical Society, 1998.

[16] R. Rosencranz and S. A. Bogen, "Clinical laboratory measurement of serum, plasma, and blood viscosity," *Am J Clin Pathol*, vol. 125 Suppl, pp. 78–86, Jun 2006.

[17] S. Patankar, *Numerical Heat Transfer and Fluid Flow*, 1st ed. Hemishpere Publishing Corporation, 1980.

[18] S. Mori, B. Crain, and P. van Zijl, "3D brain fiber reconstruction from diffusion MRI," in *Proceedings of International Conference on Functional Mapping of the Human Brain*, 1998.